

ENHANCED THE DFIG SYSTEM BEHAVIOR UNDER SYMMETRICAL SAG VOLTAGE.

¹TARIQ RIOUCH, ²RACHID EL-BACHTIRI

¹USMBA University, ESTF, Technologies et Services Industriels Laboratory, Fez, Morocco, High school of technology BP 2427 Route d'Imouzzer 30000 Fez, Morocco

²USMBA University, ESTF, Technologies et Services Industriels Laboratory, Fez, Morocco, High school of technology BP 2427 Route d'Imouzzer 30000 Fez, Morocco

E-mail: ¹tariq.riouch@gmail.com, ²rachid.elbachtiri@usmba.ac.ma

ABSTRACT

This paper proposes a novel scheme to improve the low voltage ride-through (LVRT) capability of the doubly-fed induction generator (DFIG) based wind power (WT). The main problems of DFIG are; its sensitivity to voltage sag in side and the sudden variation in wind speed on the other side, these problems causes the fluctuations in the output power, overcurrent in rotor winding and overshoot in the dc bus voltage. A Hybrid Energy Storage System (HESS) connected in parallel with the rotor side converter of the DFIG, and an adequate control of the HESS are suggested to enhance the DFIG behavior. The simulations is conducting in MATLAB/Simpower system environment, The results show that the proposed scheme can not only enhanced the DFIG behavior under fault, but also smooth the power injected in grid under normal operation with the sudden variation of the wind speed.

Keywords: *Wind power generation; doubly fed induction generator (DFIG); Hybrid Energy Storage System (HESS); Voltage sag; Power fluctuation*

1. INTRODUCTION

The progress of wind turbine technology, making it very attractive to replace traditional sources, combating environmental degradation from CO₂ emissions of the traditional power plants. The increase of the integration of the wind turbines in the electricity grid this last decade has posed several problems:

- 1) The stability of the electrical system.
- 2) The fluctuations of the output power.

The wind turbine based doubly fed induction generator (DFIG) is the most used in the farms of the wind turbine. The DFIG shown in figure 1 is the most exploited in the wind energy exceeding 1 MW, thanks to these advantages; the decoupled control of active and reactive power, operation at variable speed, the powers converters are dimensioned only 25% - 30% of the rated power of the DFIG and [1]-[2].

The stator of DFIG is connected directly to electrical grid, but this rotor linked to the grid via two converters; the rotor side converter (RSC) and the grid side converter (GSC), between these two converters, we find the DC Bus. The controls of the

RSC converts is using for regulating the decoupled active and reactive power (orientation of field). The GSC converters is using to stabilizing the voltage of DC bus and to control the reactive power injected by this converter into grid.

Different classical strategies controls were employed to order DFIGs; controls vector (VC), direct control of couple (DTC) and the direct control of power (DPC) [3]-[4].

When the fault occurs in the power grid the doubly fed induction generator based wind turbine must ben remain connected to the grid electrical and contribute to the stability of the power systems. A sag voltage in stator voltage due to grid fault produces a dc component in the stator flux. this translates into; a large transient current appears in the rotor winding an the overvoltage in the DC bus which causes degradation of the DFIG performance and perturbs the behavior system, and it can damage the power converters. Not only the fault grid but also the sudden variation speed of the wind disturbs the DFIG behavior causing fluctuations in the power produced [5]-[6]-[25].

With the increased DFIG penetration in electrical grid, the DFIG performance under the

grid faults and fluctuations of the output power injected in the grid become important issues to be addressed [7]. Several strategies have been used mainly to maintain the connection of the DFIG to electrical grid.

The solutions presented for improving the LVRT capability of DFIG can be mainly divided into two categories: auxiliary hardware solutions and improved control strategies. In side the improved control strategies like stator current feedback control [17], demagnetization control [18], and inductance emulating control (IEC) [19] are only suitable for moderate voltage sags [24].

In the other side, hardware solutions such as static synchronous compensators (STATCOM) [20].

Other hardware solutions like crowbar protection circuit using a series of resistance [21], can only solve part of the LVRT problems [21]. series grid side converter (SGSC) [22], dynamic voltage restorer (DVR) [23], energy storage system (ESS) and Superconducting magnetic energy storage (SMES), which are characterizing by highly efficient energy storage and power controllability under faults [8]-[9] have good effect on enhancing LVRT capacity.

However, the LVRT methods mentioned above act during the electrical grid fault and it remains inactive in the normal operation during the sudden variation speed of the wind.

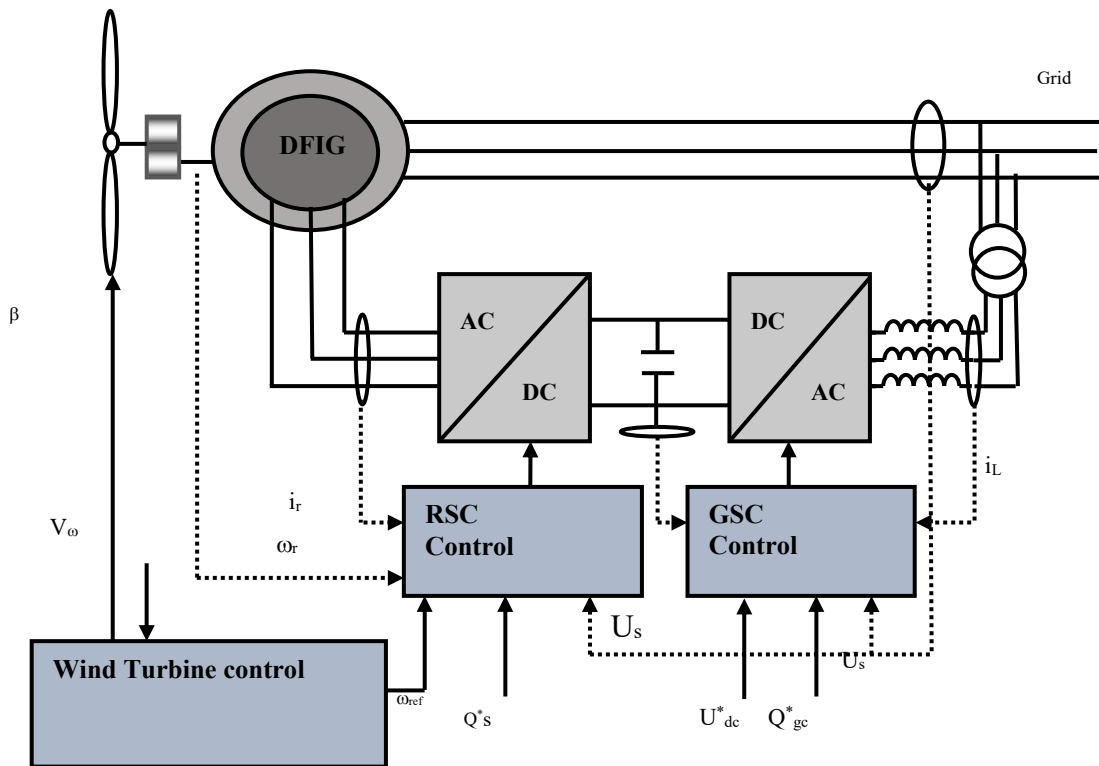


Fig. 1. Configuration of a DFIG wind turbine system

In this paper, an additional Hybrid Energy Storage System (HESS) connected in parallel with the rotor side converter of the DFIG and its control are proposed for enhanced LVRT capability under grid fault and in the normal condition with sudden speed variation of the wind.

Using MATLAB SIMULINK, the model of the HESS system for DFIG and its control strategy of the system has developed, and the simulation tests are performing to validate our proposed control.

2. DFIG MODEL UNDER GRID FAULT

The model generally used for the DFIG is the Park's model [10]. For the simplification of the study, the rotor variables will to be referring to as the stator:

$$\vec{v}_s = R_s \vec{i}_s + \frac{d}{dt} \vec{\psi}_s \quad (1)$$

$$\vec{v}_r = R_r \vec{i}_r + \frac{d}{dt} \vec{\psi}_r - j\omega \vec{\psi}_s \quad (2)$$

Where i represents the current, v the voltage, ψ the magnetic flux, ω the rotor electrical speed and R the resistance. The subscripts r and s indicate rotor and stator variables.

In the case of DFIG, the stator windings have connected directly to the grid, which means that the stator voltage v_s is determined by the grid. The rotor voltage v_r of DFIG has controlled by rotor side converter and used to perform the machine control. The stator and rotor fluxes has given by:

$$\vec{\psi}_s = L_s \vec{i}_s + L_m \vec{i}_r \quad (3)$$

$$\vec{\psi}_r = L_r \vec{i}_r + L_m \vec{i}_s \quad (4)$$

Where L_m presents the inductance magnetizing. L_s and L_r represents the stator and rotor inductance, respectively. The rotor voltage V_r is one of the most important variables for the converter. This voltage has induced by the variation of the rotor flux, which is calculated by (3) and (4):

$$\vec{v}_r = \frac{L_m}{L_s} \frac{d\vec{\psi}_s}{dt} + \sigma L_r \cdot \vec{i}_r, \quad \sigma = 1 - \frac{L_m^2}{L_s L_r} \quad (5)$$

σ being the leakage factor and σL_r the rotor transient inductance.

From (2) and (5), the following expression is obtaining:

$$\vec{v}_r = \frac{L_m}{L_s} \frac{d\vec{\psi}_s}{dt} - (R_r \vec{i}_r + \sigma L_r \frac{d\vec{i}_r}{dt}) \quad (6)$$

The rotor voltage given by (6) showed two items. The first will be referred to as EMF it is induced by the stator flux and the second item is the voltage drop caused by the rotor current in both rotor transient inductance σL_r and the rotor resistance R_r .

During normal operation, neglecting the stator resistance R_s , the stator flux linkage can be expressed as [11].

$$\vec{\psi}_s = \frac{V_s}{j\omega_s} e^{j\omega_s t} \quad (7)$$

Where ω_s is the stator angular frequency, V_s is the amplitude of stator voltage. Then the EMF induced by the stator flux linkage during normal condition can be calculating according to (6)

$$\vec{e}_r = \frac{L_m}{L_s} \frac{d}{dt} \vec{\psi}_s = \frac{L_m}{L_s} s V_s e^{j\omega_s t} \quad (8)$$

Where s is the slip, and $\omega_s r$ is slip angular frequency. The amplitude of the EMF e_r is $sV_s L_m / L_s$, which is proportional to the slip s . typically; s is variable between -0.3 and 0.3 , so the EMF under normal condition is relatively small.

Under symmetrical fault occurs, the stator flux linkage would contain DC component, and can be expressed as [11],[12].

$$\vec{\psi}_s = \frac{V_s(1-p)}{j\omega_s} e^{j\omega_s t} + \frac{V_s p}{j\omega_s} e^{-\frac{t}{\tau_s}} \quad (9)$$

Where p is the depth of voltage dip, and τ_s is the time constant of the stator flux linkage. The first item is the positive sequence component of the stator flux linkage, and the second item is the DC component, which decays with the time constant τ_s . Then according to (6), the EMF under symmetrical faults can be giving by:

$$\vec{e}_r = \frac{L_m}{L_s} \left[s V_s (1-p) e^{j\omega_s t} - V_s p (1-s) e^{-j\omega_s t} e^{-\frac{t}{\tau_s}} \right] \quad (10)$$

3. HESS CONTROL APPROACHES

3.1 description of system

The main circuit of DFIG and the additional (HESS) system is showing in Fig. 2. The DC link system is composed of RSC, GSC, DC chopper, and HESS. The energy stored in the HESS enables an exchange of active power with the system for a short period.

This controller could be using to improve the regulation of the real power flow of a wind farm. The energy storage system is previously been used to improve the power supply reliability for industrial customer [12]-[13].

The idea of the mentioned control strategies is the battery are used to supports the average power fluctuation, and the SC is used to improve the dynamic high-frequency power fluctuations. However, the error of the current present of the battery system, due to response dynamics of the battery, battery controller, and bi-directional DC-DC converter is not sufficiently studying in control strategies. To solve the mentioned problems, a joint control strategy is proposing in this article, which provides faster DC link voltage restoration compared to conventional control strategies.

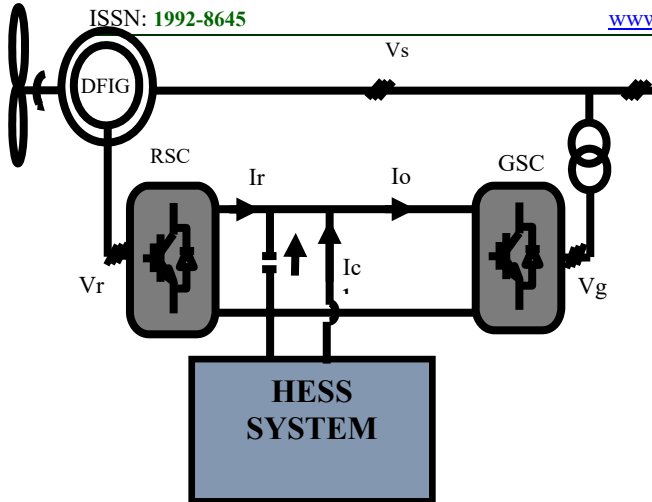


Figure 2. The main circuit of DFIG wind power system based on HESS.

This controller could be using to improve the regulation of the real power flow of a wind farm. The energy storage system is previously been used to improve the power supply reliability for industrial customer [12]-[13].

The idea of the mentioned control strategies is the battery are used to supports the average power fluctuation, and the SC is used to improve the dynamic high-frequency power fluctuations. However, the error of the current present of the

battery system, due to response dynamics of the battery, battery controller, and bi-directional DC-DC converter is not sufficiently studying in control strategies. To solve the mentioned problems, a joint control strategy is proposing in this article, which provides faster DC link voltage restoration compared to conventional control strategies.

The proposed control strategy utilizes the power from the battery system to overtake the slow response dynamics, which includes bidirectional DC-DC converter, battery monitor and battery dynamics. The proposed system and control also helps to improve the battery lifetime. The advantages of our proposed scheme approach are:

- 1) Faster response of DC link voltage restoration.
- 2) Less stress in energy storage system.
- 3) Suppress the overvoltage in DC link voltage.

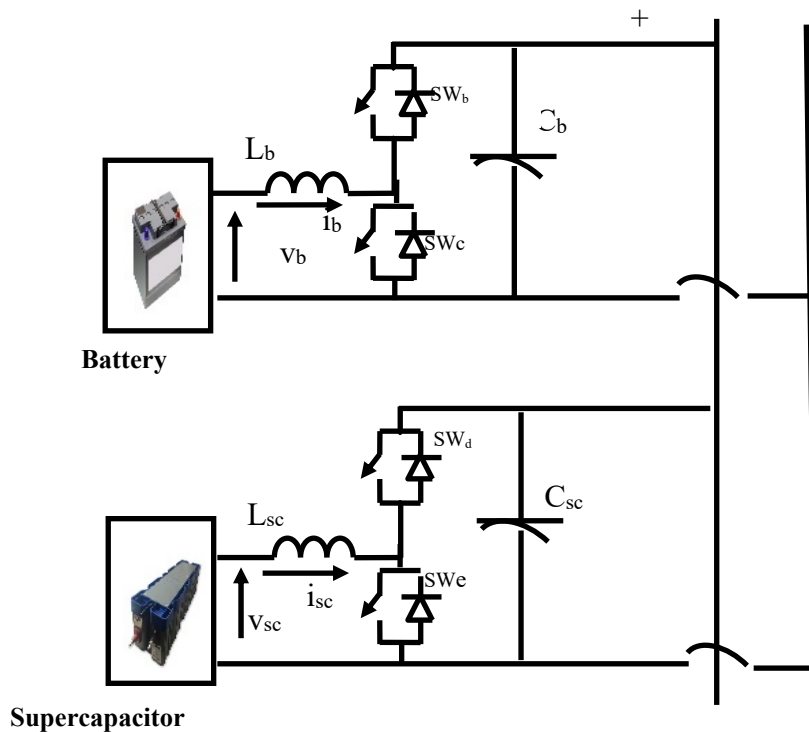


Figure .3. Architecture of the proposed HESS System

The overall configuration of the HESS studied in this paper is represented in Fig. 3. The HESS include two energy storage systems; battery and super-capacitor. The DC link of the DFIG is connected the DC bus of HESS using a unidirectional DC-DC boost converter.

The HESS presented is effective in supplying the average power demand for a long duration, and transient power fluctuations for short duration. In Fig. 3, vsc and vbatt are SC and battery terminal voltage respectively, Lsc and Lbatt are inductor parameters for SC, and battery. Csc and Cbatt are the filter capacitance of battery and SC converter. sw_a, sw_b, sw_c, sw_d and sw_e are representation of the control switches used for DC-DC converters. The ibatt, isc represent the battery, SC respectively. The DC link voltage is representing as V_{dc}.

3.2 Proposed Control and stability Analysis.

The proposed control is showing in Fig. 4. The proposed control is to reduce the stress on the battery and, to restore the DC link voltage as fast as possible, thus increasing the operating life of the battery system. Unlike the conventional control strategy [14]-[15], the power required to smooth and to balance the overall power flow in the DC link during load and generation variation is categorized into two components, (i) average power component (P_m), and (ii) transient power components (P_{tr}). The power balance equation can be stating as follows,

$$P_{GSC}(t) - P_{RSC}(t) = P_b(t) + P_{sc}(t) = \bar{P}_m + \hat{P}_{tr} \quad (11)$$

Where, P_{sc}(t), P_b(t), P_{rsc}(t) and P_{gsc}(t) are SC, battery, rotor side converter and grid side converter power respectively.

In order to maintain the DC link voltage at certain level, the net power required to be supplying by the HESS is given by (2)

$$\bar{P}_m(t) + \hat{P}_{tr}(t) = v_{dc} i_T \quad (12)$$

The total current of the HESS to maintain a constant DC link voltage is:

$$i_T(t) = \left(\frac{\bar{P}_m}{v_{dc}}\right) + \left(\frac{\hat{P}_{tr}}{v_{dc}}\right) = \bar{i}_m(t) + \hat{i}_{tr}(t) \quad (13)$$

A total current i_T (t) is obtaining from the voltage control loop and it is given in

$$i_T(t) = \bar{i}_m(t) + \hat{i}_{tr}(t) = K_{p-vdc} v_{er} + k_{i-vdc} \int v_{er} dt \quad (14)$$

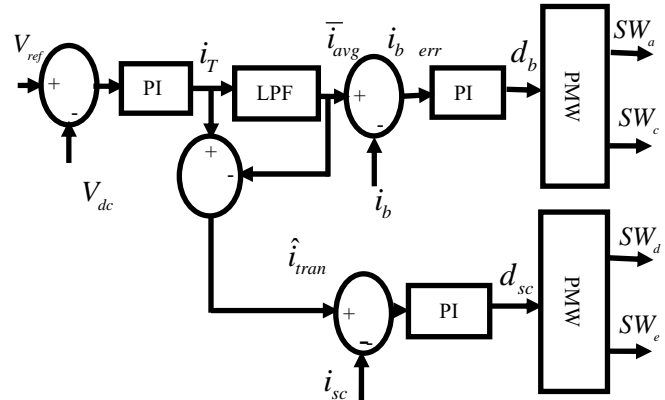


Fig. 4. Proposed control strategy

Where K_{i_Vdc} and K_{p_vdc} are the integral and the proportional coefficient of the voltage control loop, where V_{er}, V_{ref} and V_{dc} are the error voltage, DC link voltage reference and measured DC link voltage respectively. The effective sharing of i_T is essential to achieve a faster DC link voltage restoration and effective performance of the proposed control strategy. As in conventional control strategy, LPF is employing to extract an average component from i_T. (5) give the average current (i_m),

$$i_{bref}(s) = \bar{i}_{avg}(s) = \frac{\omega_s}{s + \omega_s} i_T(s) \quad (15)$$

Where i_{bref} (s) and ω_c are the cut-off frequency of the LPF and the reference current for the battery converter control. The LPF cut-off frequency is chosen to be 2π*5 rad/sec. The average current is controlling by the system of the battery. Due to the slow response of the battery system, which includes dynamics of the battery, battery controller and bidirectional DC-DC converter.

The actual current is comparing to the generated battery and SC reference currents. The error is then fed to the PI current control, which generates a duty ratio to follow the reference current.

The objective of the proposed strategy is to regulate the DC link voltage as fast as possible, while maintaining the proper power flow balance in the DC link. The dynamic behavior of the HESS during supply and demand depends on the SC, battery and RSC current response to the change in the DC link voltage.

3.3 SC Current Control Loop Design

$$G_{ol_sc} = G_{pi_sc} G_{id_sc} H_{sc} \quad (16)$$

The open loop transfer function (G_{ol_sc}) and closed loop transfer function (G_{cl_sc}) of the SC current control loop are giving below,

$$G_{ol_sc} = \frac{G_{pi_sc} G_{id_sc}}{1 + G_{pi_sc} G_{id_sc} H_{sc}} \quad (17)$$

K_{i_sc} and K_{p_sc} are the integral gain and the proportional gain for the SC current control loop respectively. H_{sc} represents the feedback gain for the SC current control loop. The SISO toolbox in Matlab is used to design the controller parameters. The controller parameters obtained for the SC current control loop are, $K_{p_sc} = 0.52$ and $K_{i_sc} = 1800$.

3.4 Battery Current Control Loop Design

The open loop transfer function (G_{ol_b}) of the battery current control loop is giving below,

$$G_{ol_b} = G_{pi_b} G_{id_b} H_b \quad (18)$$

K_{p_b} and K_{i_b} are the proportional and integral gain for the battery current control loop respectively. In (21), H_b is the feedback gain of the battery current control loop. The bode plot of the open loop transfer function for battery current control loop is shown in Fig. 4(c). The SISO toolbox in Matlab [16] is used to design the controller parameters. The controller parameters obtained for the battery current controller loop are $K_{p_b} = 0.23$ and $K_{i_b} = 2100$.

4. SIMULATION RESULTS

To evaluate the system performance, the model of the SMES based excitation system for DFIG is establishing using MATLAB SIMULINK. The model contains a six DFIG wind turbine. According to the system parameters of the electric power system dynamic simulation laboratory, the parameters DFIG are designing as shown in Table I.

Fig.7 represents the rotor current of DFIG with the conventional control under the faults. Fig. 8 show the quick response by reduction of the peak of the rotor current with the proposed strategy. By

introducing the HESS into the DC link system of DFIG, the active power which is smoothen as shown in fig. 9, the fluctuation is smoothed precisely between $t_i=0.8s$ and $t_f=1.4s$. Fig.10 represents the reactive power of DFIG with the conventional strategy and with the proposed strategy. We can see that it is superior to zero this can enhanced the system stability by the injection of the reactive power. Fig.11. shows the fluctuations of the DC bus voltage with conventional strategy, which could reach 1425 V; this may destroy the power converters and destabilizes the dynamic performance of DFIG. With the proposed strategy, the DC bus voltage become more stable with slight fluctuations compared to overshoot of the DC bus voltage observed with conventional strategy.

Comparative performance evaluation of the proposed and the conventional strategy under long-term and short-term scenario are carrying out. The short-term performance analysis is performing to study the capability of the proposed scheme and its control to deal with sudden changes in the generation.

Table 1. Transfer functions for control of Hess System

Duty Cycle to inductor current transfer function for SC
$G_{id_sc} = \frac{\bar{i}_{sc}}{d_{sc}} = \frac{(C_{sc} v_{dc})s + 2(1 - d_{sc})i_L}{(L_{sc} C_{sc})s^2 + \frac{L_{sc}}{R}s + (1 - d_{sc})^2}$
Inductor current to output voltage transfer function for SC
$G_{iv_sc}(s) = \frac{\hat{v}_{dc}}{\hat{i}_{sc}} = \frac{(1 - d_{sc})v_{dc} - (L_{sc} i_L)s}{(C_{sc} v_{dc}) + 2(1 - d_{sc})i_L}$
Duty Cycle to inductor current transfer function for battery
$G_{id_sc}(s) = \frac{i_b}{d_b} = \frac{(c_b v_{dc})s + 2(1 - d_b)i_L}{(L_b C_b)s^2 + \frac{L_b}{R}s + (1 - d_b)^2}$

Table 2. Specifications Used For the Simulation

Components	Part name	Rating values
DFIGs	Rated Generator Power	6×1,5 MW
Vs	Rated Terminal stator voltage	690 V
f	Rated frequency	50 Hz
Rs	Stator Resistance	0.0048 mΩ
Ls	Stator leakage inductance	0.1386 mH
Rr	Rotor Resistance	0.00549 mΩ
Lr	Rotor leakage inductance	0.1493 mH
Vdc	Rated DC-link Voltage	1150 V
Cd	Input Capacitance	10μF
L	SC Inductor	2.5 H
fs	Switching Frequency	10 KHZ
Kp	Proportional coefficient	0.1128
Ti	Integral coefficient	0.12

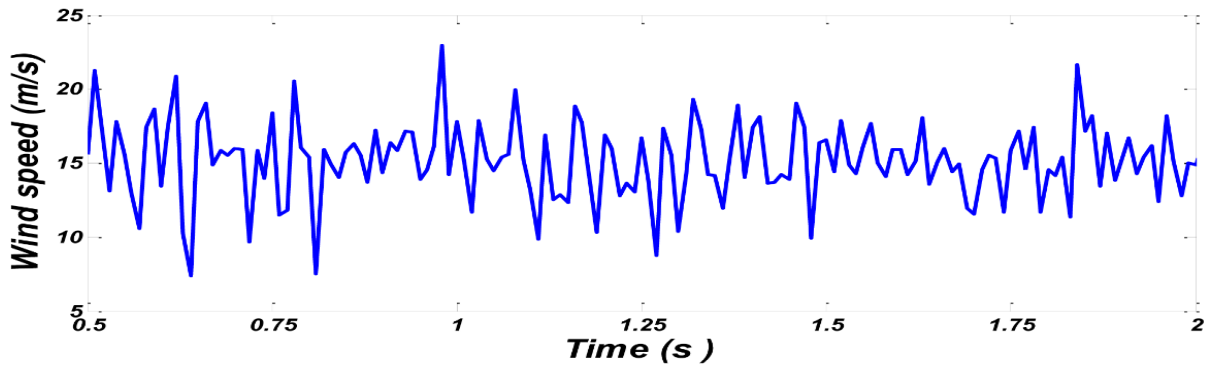


Fig.5. Wind speed evolution

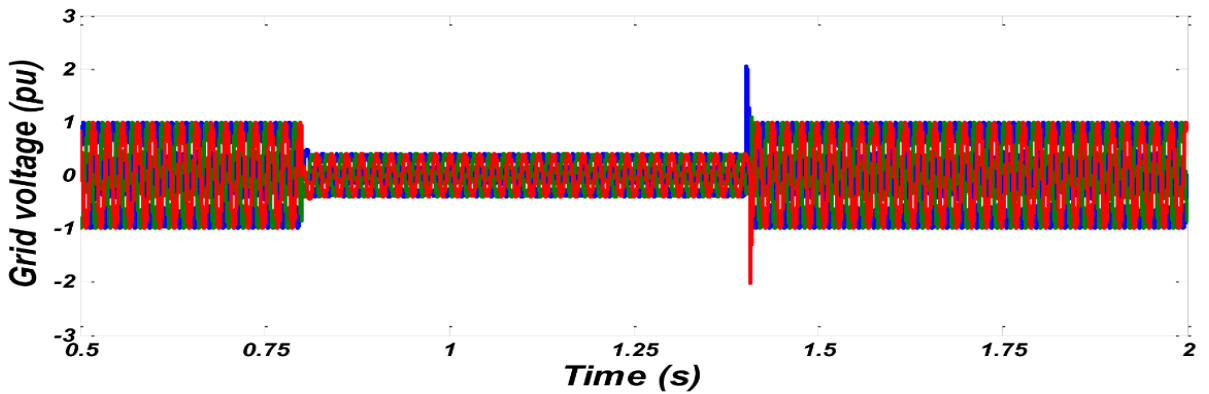


Fig.6. Grid voltage

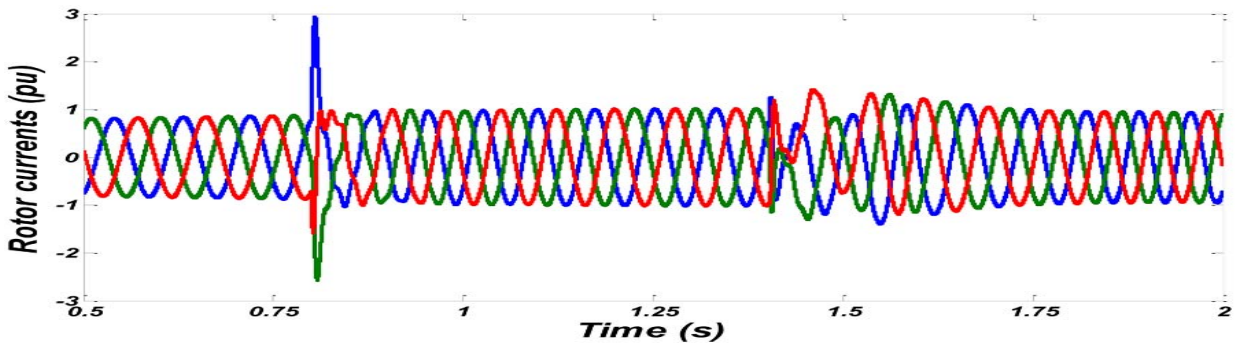


Fig.7. Rotor current without the proposed control

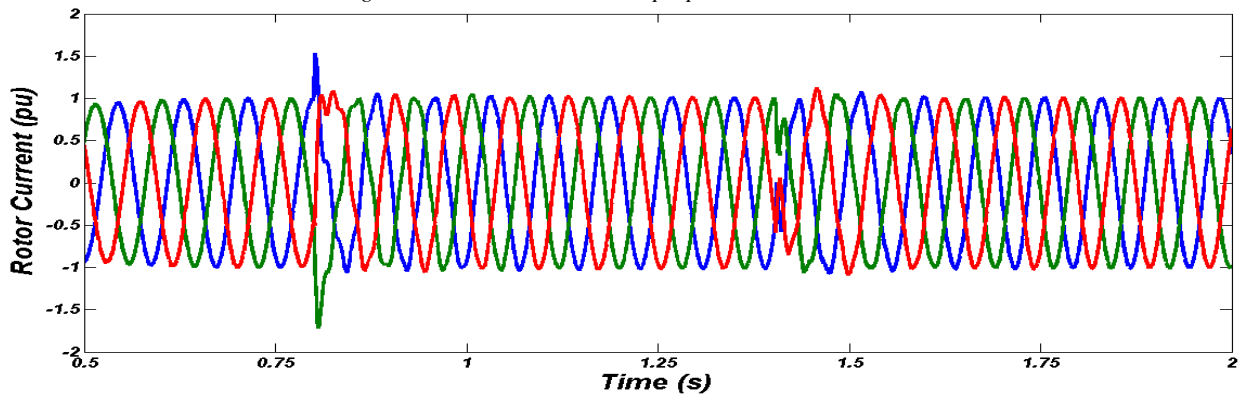


Fig.8. Rotor current with the proposed control

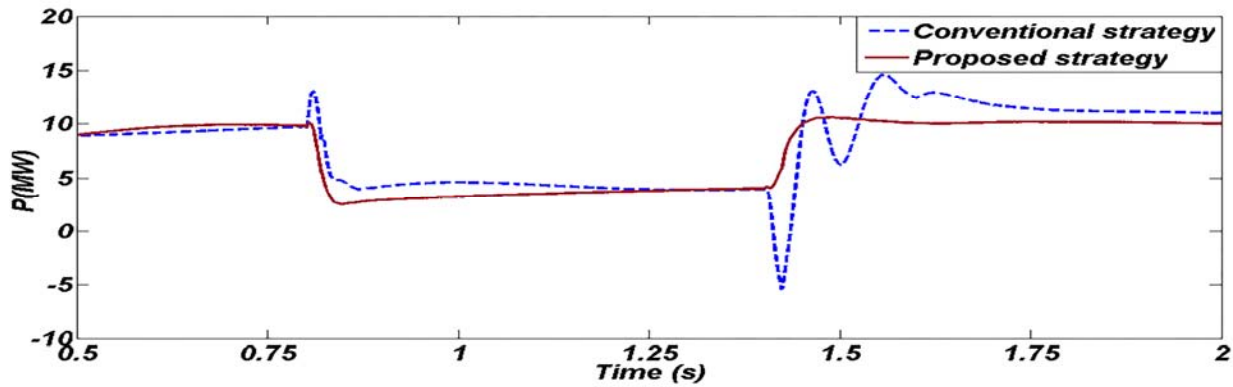


Figure.9. Output active power

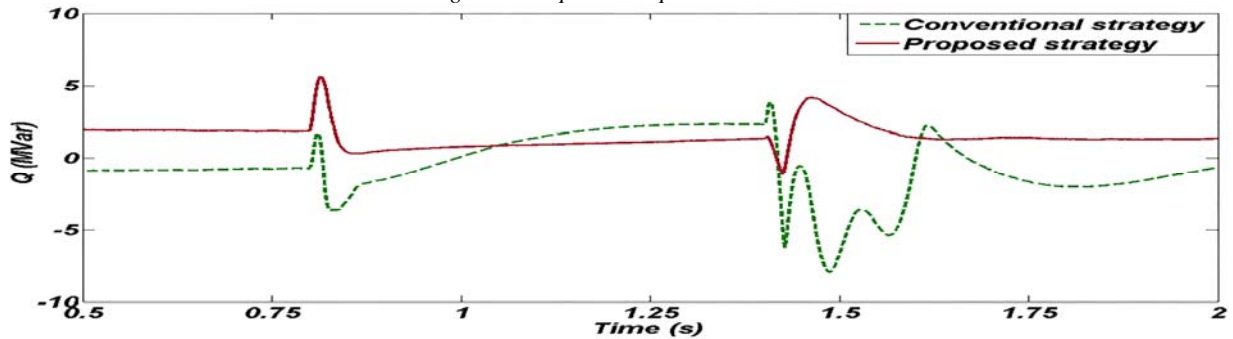


Figure.10. Output reactive power

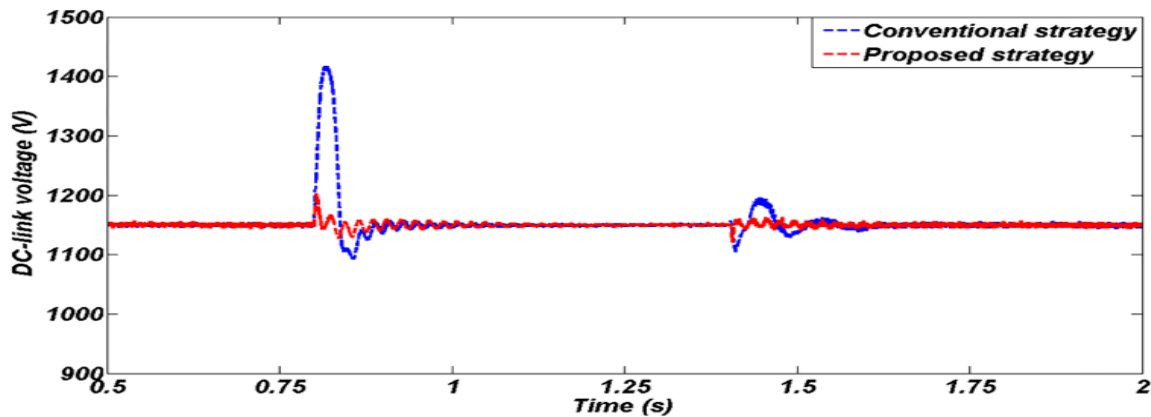


Figure. 11. DC-link voltage

The comparison was made between the two schemes; conventional scheme with a battery and our proposed scheme, that it is composed of a battery and a super-capacitor.

The results obtained clearly show the effectiveness of the proposed system. This can be seen on the smoothing of the active and reactive power, the reductions peaks of the over current in the rotor winding and the overshoot of the DC bus voltage.

5. CONCLUSION

The proposed novel scheme and its control are presented in this paper. The effects of the proposed LVRT of the DFIG has been verified in a 6×1.5 MW DFIG-based wind farms. The simulations results showed the comparison between conventional and the proposed schemes in the normal operation of the electrical grid and under symmetrical faults has been showing.

We can clearly see in figure 8, figure 9 and figure 10 the improvement in the rotor current evolution, and the smoothen active and reactive power respectively. the elimination of the DC bus voltage fluctuations can be seen in figure 11. These simulations have been verified during normal condition and under disturbed regime.

To have a broad view, our future work will deal with the proposed system during an asymmetric fault.

REFERENCES

- [1] J. Liang, W. Qiao and R.G Harley, "Feed-Forward Transient Current Control for Low-Voltage Ride-Through Enhancement of DFIG Wind Turbines" IEEE Trans. on energy Conversion, vol. 25,(Issue 3), 836843,September2010.
- [2] S. Hu, X. Lin, Y. Kang, and X. Zou, "An improved low-voltage ride-through control strategy of doubly fed induction generator during grid faults" IEEE Transactions Power Electron., 2011, 26, (Issue12): 36533665, December 2011.
- [3] E.Tremblay, S.Atayde and A.Chandra, "Comparative Study of Control Strategies for the Doubly Fed Induction Generator in Wind Energy Conversion Systems: A DSP-Based Implementation Approach", IEEE Trans. Sustainable energy, vol. 2,(Issue 3), 288-299, July 2011.
- [4] Tariq Riouch, Rachid El-Bachtiri and Mohamed Salhi "Robust Sliding Mode Control for Smoothing the Output Power of DFIG under Fault Grid" International Review on Modelling and Simulations (IREMOS), Vol.6, no.4, pp 1264-1270, August 2013.
- [5] T. Riouch and R. El-Bachtiri "Advanced Control Strategy of Doubly Fed Induction Generator Based Wind-Turbine during Symmetrical Grid Fault" International Review of Electrical Engineering (IREE) Vol 9, No 4 (2014).
- [6] W.Guo, L.Xiao, and Shaotao Dai, "Enhancing Low-Voltage Ride-Through Capability and Smoothing Output Power of DFIG With a Superconducting Fault-Current Limiter–Magnetic Energy Storage," IEEE Trans. Energy convers, vol. 27, no. 2, pp.277-295, June 2012.
- [7] T. Riouch, R. EL-Bachtiri, A. Alamery and C. Nichita, "Control of Battery Energy Storage System for Wind Turbine based on DFIG during Symmetrical Grid Fault" In

- Proc. The International Conference on Renewable Energies and Power Quality (ICREPQ'15), 25th to 27th March, 2015.
- [8] A. Abu-Siada and S. Islam, "Application of SMES Unit in Improving the Performance of an AC/DC Power System," *Sustainable Energy*, IEEE Transactions on, vol. 2, pp. 109-121, 2011.
- [9] S. Jing, T. Yuejin, X. Yajun, R. Li, and L. Jingdong, "SMES based excitation system for doubly-fed induction generator in wind power application," *IEEE Trans. Appl. Supercond.*, vol. 21, no. 3, pp. 1105-1108, Jun. 2011.
- [10] J. Lopez, P. Sanchis, X. Roboam, and L. Marroyo, "Dynamic behavior of the doubly-fed induction generator during three-phase voltage dips," *IEEE Trans Energy Convers.*, vol. 22, no. 3, pp. 709-717, Sep. 2007.
- [11] S. Xiao, G. Yang, H. Zhou and H. Geng, "A LVRT Control Strategy based on Flux Linkage Tracking for DFIG-based WECS" *IEEE Trans. Ind. Electron.*, vol. 60, no. 7, pp.2820 -2832 2013.
- [12] Kolluri, S.; "Application of distributed superconducting magnetic energy storage system (D-SMES) in the energy system to improve voltage stability" *Power Engineering Society Winter Meeting, 2002. IEEE*, Volume: 2, 2002. Page(s): 838 -841 vol.2.
- [13] Ross, M.; Borodulin, M.; Kazachkov, Y.; "Using D-SMES devices to improve the voltage stability of a transmission system" *Transmission and Distribution Conference and Exposition, 2001 IEEE/PES*, Volume: 2,2001. Page(s): 1144 -1148 vol.2.
- [14] H. Zhou, T. Bhattacharya, D. Tran, T. S. T. Siew, and A. M. Khambadkone, "Composite energy storage system involving battery and ultracapacitor with dynamic energy management in microgrid applications," *IEEE Transactions on Power Electronics*, vol. 26, no. 3, pp. 923-930, Mar. 2011.
- [15] M. Hamzeh, A. Ghazanfari, Y. A. R. I. Mohamed, and Y. & Karimi, "Modeling and design of an oscillatory current-sharing control strategy in dc microgrids," *IEEE Transactions on Industrial Electronics*, vol. 62, no. 11, pp. 6647-6657, Nov. 2015.
- [16] Q. Xu, J. Xiao, P. Wang, X. Pan, and C. Wen, "A decentralized control strategy for autonomous transient power sharing and state-of-charge recovery in hybrid energy storage systems," *IEEE Transactions on Sustainable Energy*, vol. PP, no. 99, pp. 1-1, 2017.
- [17] F. K. A. Lima, A. Luna, P. Rodriguez, E. H. Watanabe and F. Blaabjerg, "Rotor Voltage Dynamics in the Doubly Fed Induction Generator During Grid Faults," *IEEE Trans. Power Electron.*, vol. 25, no. 1, pp. 118-130, Jan. 2010.
- [18] D. W. Xiang, L. Ran, P. J. Tavner and S. Yang, "Control of a doubly fed induction generator in a wind turbine during grid fault ride-through," *IEEE Trans. Energy Convers.*, vol. 21, no. 3, pp. 652-662, Sept. 2006.
- [19] Q. Huang, X. Zou, D. Zhu and Y. Kang, "Scaled current tracking control for doubly fed induction generator to ride-through serious grid faults," *IEEE Trans. Power Electron.*, vol. 31, no. 3, pp. 2150-2165, March 2016.
- [20] Y. Kailasa Gounder, D. Nanjundappan and V. Boominathan, "Enhancement of transient stability of distribution system with SCIG and DFIG based wind farms using STATCOM," *IET Renew. Power Gener.*, vol. 10, no. 8, pp. 1171-1180, Sept. 2016.
- [21] M. M. Hossain and M. H. Ali, "Transient stability improvement of doubly fed induction generator based variable speed wind generator using DC resistive fault current limiter," *IET Renew. Power Gener.*, vol.10, no. 2, pp. 150-157, 2 2016.
- [22] P. S. Flannery and G. Venkataramanan, "Unbalanced Voltage Sag Ride-Through of a Doubly Fed Induction Generator Wind Turbine With Series Grid-Side Converter," *IEEE Trans. Ind. Appl.*, vol. 45, no. 5, pp.1879-1887, Sept.-oct. 2009.
- [23] D. Ramirez, S. Martinez, C. A. Platero, F. Blazquez and R. M. de Castro, "Low-voltage ride-through capability for wind generators based on dynamic voltage restorers," *IEEE Trans. Energy Convers.*, vol. 26, no. 1, pp. 195-203, March 2011.
- [24] X. Xiao, R. Yang, Z. Zheng and Y. Wang, "Cooperative Rotor-Side SMES and Transient Control for Improving the LVRT Capability of Grid-Connected DFIG-Based Wind Farm," *IEEE Trans. on Applied Superconductivity*, vol. 29, no. 2, pp. 1-5, March 2019.
- [25] Tariq RIOUCH and Rachid EL-BACHTIRI "Improved DFIG System Behavior With Smes System During Voltage Sag" *Journal of Theoretical and Applied Information Technology JATIT*, pp. 696-705, Vol. 99 No.3, 15th February 2021.